Cell PRESS
Neuron
Article

Activity-Dependent Proteolytic Cleavage of Neuroligin-1

Kunimichi Suzuki,[1] Yukari Hayashi,[1] Soichiro Nakahara,[2] Hiroshi Kumazaki,[3] Johannes Prox,[5] Keisuke Horiuchi,[6] Mingshuo Zeng,[3] Shun Tanimura,[3] Yoshitake Nishiyama,[3] Satoko Osawa,[1] Atsuko Sehara-Fujisawa,[7] Paul Saftig,[5] Satoshi Yokoshima,[3] Tohru Fukuyama,[3] Norio Matsuki,[2] Ryuta Koyama,[2] Taisuke Tomita,[1,8,*] and Takeshi Iwatsubo[1,4,8]
[1]Department of Neuropathology and Neuroscience
[2]Laboratory of Chemical Pharmacology
[3]Laboratory of Synthetic Natural Products Chemistry, Graduate School of Pharmaceutical Sciences
[4]Department of Neuropathology, Graduate School of Medicine
The University of Tokyo, Hongo 7-3-1, Bunkyo, Tokyo 113-0033, Japan
[5]Institut für Biochemie, Christian-Albrechts-Universität zu Kiel, D-24098 Kiel, Germany
[6]Department of Orthopedic Surgery, School of Medicine, Keio University, Shinjuku, Tokyo 160-8582, Japan
[7]Department of Growth Regulation, Institute for Frontier Medical Sciences, Kyoto University, Sakyo-ku, Kyoto 606-8507, Japan
[8]Core Research for Evolutional Science and Technology, Japan Science and Technology Agency
*Correspondence: taisuke@mol.f.u-tokyo.ac.jp
http://dx.doi.org/10.1016/j.neuron.2012.10.003

SUMMARY

Neuroligin (NLG), a postsynaptic adhesion molecule, is involved in the formation of synapses by binding to a cognate presynaptic ligand, neurexin. Here we report that neuroligin-1 (NLG1) undergoes ectodomain shedding at the juxtamembrane stalk region to generate a secreted form of NLG1 and a membrane-tethered C-terminal fragment (CTF) in adult rat brains in vivo as well as in neuronal cultures. Pharmacological and genetic studies identified ADAM10 as the major protease responsible for NLG1 shedding, the latter being augmented by synaptic NMDA receptor activation or interaction with soluble neurexin ligands. NLG1-CTF was subsequently cleaved by presenilin/γ-secretase. Secretion of soluble NLG1 was significantly upregulated under a prolonged epileptic seizure condition, and inhibition of NLG1 shedding led to an increase in numbers of dendritic spines in neuronal cultures. Collectively, neuronal activity-dependent proteolytic processing of NLG1 may negatively regulate the remodeling of spines at excitatory synapses.

INTRODUCTION

Formation and maintenance of the synaptic structure is a dynamic process that requires bidirectional interactions between pre- and postsynaptic components. A diverse assortment of cell adhesion molecules is present at the synapse and organizes the synaptic specializations of both excitatory and inhibitory central synapses (Dalva et al., 2007; Siddiqui and Craig, 2011). Neuroligin (NLG) is one of the potent synaptogenic adhesion proteins located at the postsynapse, which transsynaptically binds to a presynaptic ligand, neurexin (NRX) (Ichtchenko et al., 1995; Irie et al., 1997; Scheiffele et al., 2000; Südhof, 2008; Bottos et al., 2011). Mammals express four NLG genes (i.e., NLG1 to NLG4). NLG polypeptides are type 1 transmembrane proteins with a large extracellular domain with homology to acetylcholinesterases but lack critical residues in the active site and interact with NRXs at the synaptic membrane surface (Südhof, 2008). Notably, NLG1 is localized at glutamatergic postsynapse, and overexpression of NLG1 induces the accumulation of glutamatergic presynapse and postsynapse molecules in vitro (Song et al., 1999; Scheiffele et al., 2000; Budreck and Scheiffele, 2007). In contrast, NLG2 triggers the maturation of GABAergic synapses, implicating specific functions of different NLGs in the formation and maturation of different chemical types of synapses in vitro and in vivo (Graf et al., 2004; Varoqueaux et al., 2004, 2006).

Recent studies revealed that copy number variation or point mutation in NLG genes are linked to autism spectrum disorder (ASD), schizophrenia, or mental retardation (reviewed in Südhof, 2008). Notably, ASD-linked mutations in NLG genes have been shown to affect the expression, folding, or dimerization of NLG proteins to compromise their surface expression and binding to NRXs (Comoletti et al., 2004; Levinson and El-Husseini, 2007; Zhang et al., 2009). Moreover, copy number variations that are associated with an increased risk of ASD were identified in NLG1 locus (Glessner et al., 2009). NLG1 knockout (KO) or transgenic mice showed synaptic dysfunctions and ASD-like behaviors (Varoqueaux et al., 2006; Chubykin et al., 2007; Blundell et al., 2010; Dahlhaus et al., 2010). Thus, the levels of NLGs within the synaptic membranes are presumed to directly modulate the synaptic functions in vivo. Although several reports indicated that the surface levels of NLG1 are regulated by synaptic activities through membrane trafficking (Schapitz et al., 2010; Thyagarajan and Ting, 2010), the regulatory mechanisms to control protein levels of NLG remains unclear. Here, we show that NLG1 is sequentially cleaved by ADAM10 and γ-secretase to release its extra- and intracellular domain fragments, respectively. Proteolytic processing of NLG1 resulted in the elimination of NLG1 on the cell surface, thereby causing a decrease in the

synaptogenic activity of NLG1. We further show that ADAM10-mediated shedding is regulated in an activity-dependent manner through NMDA receptor (NMDAR) activation or by binding to secreted forms of NRXs. Our present results suggest that neuronal activity and interaction with NRXs regulate the levels of NLG1 via proteolytic processing to modulate the adhesion system as well as the functions of synapses.

RESULTS

Proteolytic Processing of NLGs in Brains and Neuronal Cultures

NLGs are synaptogenic type 1 transmembrane proteins that harbor large extracellular domains (Ichtchenko et al., 1995). While the levels of NLGs are presumed to be correlated with their physiological and pathological functions (Varoqueaux et al., 2006; Chubykin et al., 2007; Glessner et al., 2009; Blundell et al., 2010; Dahlhaus et al., 2010), little information is available on the proteolytic mechanism of NLGs. Several lines of evidence have indicated that a subset of type 1 transmembrane proteins are processed by sequential cleavages by ectodomain shedding and intramembrane cleavage, the latter being executed by γ-secretase (Beel and Sanders, 2008; Bai and Pfaff, 2011). To test whether the levels of NLGs are regulated by proteolytic processing, we analyzed endogenous NLG polypeptides in adult rat brains (Figure 1A). Immunoblot analysis using antibodies that specifically recognize the cytoplasmic region of NLG1 and NLG2 (see Figure S1 available online) revealed immunopositive bands at ~20–25 kDa, in addition to full-length (FL) protein that migrated at ~120 kDa. Because the predicted sizes of the cytoplasmic domain of NLGs were within the range of 120–165 amino acid (aa) lengths (NLG1, 125 aa; NLG2, 137 aa), we reasoned that the ~20–25 kDa polypeptides represent the membrane-tethered C-terminal fragment (CTF) of endogenous NLGs. Multiple bands corresponding to CTFs may represent different posttranslational modifications (e.g., glycosylation, see below). To examine whether these CTFs are processed by the γ-secretase activity, we incubated the membrane fractions of rat brains at 37°C and detected the appearance of additional bands that migrate faster than the CTFs with each NLG. Moreover, addition of DAPT, a specific γ-secretase inhibitor, abolished the generation of the smaller CTFs, in a similar manner to that observed with a well-known γ-secretase substrate, amyloid precursor protein (APP). These data suggested that NLG-CTFs are cleaved by the γ-secretase activity to release the intracellular domain (ICD) (Figure 1B). In parallel with the generation of ICDs, we observed a significant reduction in NLG1-FL upon incubation, concomitant with the generation of a smaller NLG1 fragment, which was detected by an antibody against the extracellular region of NLG1 (Figure 1C). Generation of this extracellular fragment of NLG1 was decreased by treatment with metalloprotease inhibitors (i.e., EDTA, TAPI2), supporting the notion that the extracellular domain of NLG1 is processed by ectodomain shedding. To test whether this processing occurs at synapses under a physiological condition, we incubated synaptoneurosome preparation from adult mouse brain, which contains a population of purified presynaptic boutons attached to postsynaptic processes (Villasana et al., 2006; Kim et al., 2010) (Figures 1D and 1E). After ultracentrifugation after incubation, soluble NLG1 (sNLG1) as well as NLG1-ICD was detected in the soluble fraction, which was abolished by coincubation with TAPI2 and DAPT, respectively. To ascertain that these cleavages occur in situ in neuronal cultures, we analyzed cell lysates and conditioned media (CM) from mouse cortical primary neuronal cultures obtained from embryonic day (E) 18 pups by immunoblotting and detected the secretion of an ~98 kDa single polypeptide in the conditioned media, which migrated at an identical position to that generated upon incubation of the membrane fractions, by an antibody against the extracellular domain of NLG1 (Figures 1F and 1G). This band disappeared by treatment with metalloprotease inhibitors (i.e., GM6001, TAPI2). These data suggest that the extracellular domain of NLG1 is shed by the metalloprotease activity to release sNLG1 into the conditioned media. Furthermore, DAPT treatment caused the accumulation of CTFs of NLG1 as well as of NLG2. Notably, simultaneous administration of DAPT and metalloprotease inhibitors decreased the accumulation of the CTFs. However, endogenous NLG-ICD, which was observed upon incubation of microsomes from brain lysates, was hardly detectable in cell lysates from cultured primary neurons. This suggests that NLG-ICD is a highly labile endoproteolytic product. These findings led us to speculate that NLGs are initially processed by metalloprotease at the extracellular region to generate sNLG and membrane-tethered NLG-CTF, the latter being further cleaved by the γ-secretase activity (Figure 1H).

ADAM10 and γ-Secretase Are Responsible for the Proteolytic Processing of NLG1

Next we analyzed the metabolism of NLGs in mouse embryonic fibroblasts from *Psen1*$^{-/-}$/*Psen2*$^{-/-}$ double knockout mice (DKO cells), which completely lacks the γ-secretase activity (Herreman et al., 2000). Accumulation of NLG-CTFs was observed upon the overexpression of hemagglutinin (HA)-tagged NLGs in DKO cells (Figure 2A). However, the levels of the accumulated NLG-CTFs were significantly reduced by the coexpression of human PS1, indicating that γ-secretase activity is responsible for the processing of NLG-CTFs. ADAM10 is known as a responsible enzyme for ectodomain shedding of a subset of γ-secretase substrates (e.g., Notch, APP, cadherin, and CD44) at the membrane-proximal region of ectodomain (Saftig and Reiss, 2011). To test whether ADAM10 is involved in the processing of NLGs, we overexpressed HA-tagged NLG1 or NLG2 in murine embryonic fibroblasts (MEFs) obtained from ADAM10 knockout (*Adam10*$^{-/-}$) or heterozygous (*Adam10*$^{+/-}$) mice (Figure 2B) (Hartmann et al., 2002). In *Adam10*$^{-/-}$ MEF, the generation of sNLG1 was significantly reduced. In contrast, no change in NLG1 processing was observed in MEFs obtained from knockout mice of other ADAMs (i.e., *Adam8*$^{-/-}$, *Adam17*$^{-/-}$, *Adam19*$^{-/-}$, *Adam9*$^{-/-}$; *Adam12*$^{-/-}$;*Adam15*$^{-/-}$ [TKO]) (Zhou et al., 2004; Weskamp et al., 2006; Kawaguchi et al., 2007; Horiuchi et al., 2007). These data strongly suggest that ADAM10 is a responsible enzyme for the shedding of NLG1. Intriguingly, the level of soluble NLG2 secreted from *Adam10*$^{-/-}$ MEF was almost comparable to those from other ADAM knockout MEFs, suggesting that ADAM10 specifically cleaves NLG1 but not NLG2. These data suggest

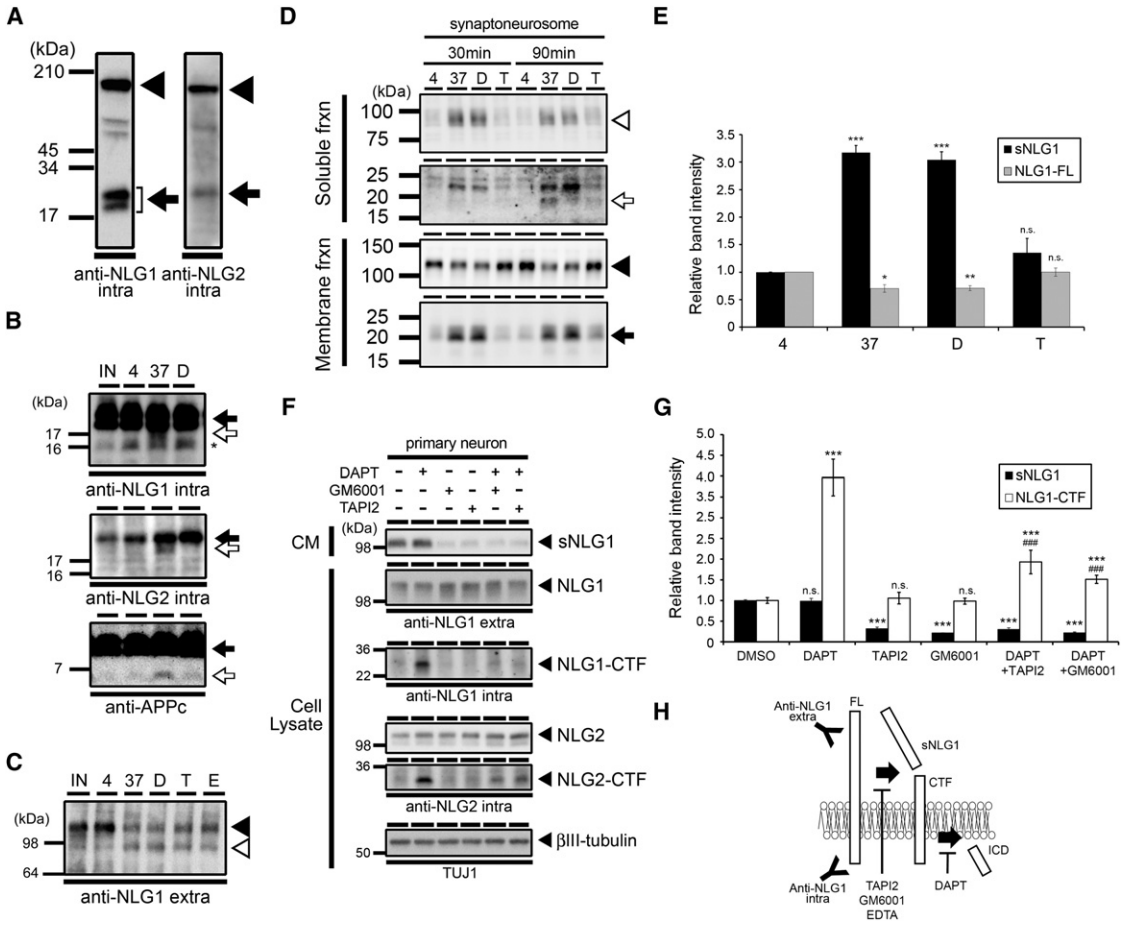

Figure 1. Proteolytic Processing of Endogenous NLGs in Rat Brains

(A) Immunoblot analysis of membrane fraction from adult rat cortex using an antibody against the intracellular domain of NLGs. Molecular weight was indicated on the left.

(B) Processing of NLG-CTFs in the cell-free assay using membrane fractions from adult rat cortex. Used antibodies are indicated below the panel. Arrows, open arrows, and asterisks represent CTFs, ICDs, and nonspecific bands, respectively. IN, input; 4, incubation at 4°C; 37, incubation at 37°C; D, incubation at 37°C with DAPT.

(C) Shedding of NLG1-FL in the cell-free assay. Arrowhead and an open arrowhead denote NLG1-FL and secreted NLG1, respectively. E, samples incubated with EDTA; T, samples incubated with TAPI2.

(D) Incubation of synaptoneurosome fraction from adult mouse brain. Open arrowhead, open arrow, arrowhead, and arrow denote sNLG1, NLG1-ICD, NLG1-FL, and NLG1-CTF, respectively. 4, incubation at 4°C; 37, incubation at 37°C; D, incubation at 37°C with DAPT; T, incubation at 37°C with TAPI2.

(E) Densitometric analysis of sNLG1 (black bar) and NLG1-FL (gray bar) in (D) (n = 3, mean ± SEM; *p < 0.05; **p < 0.01; ***p < 0.001 versus 4 degrees by Student's t test).

(F) Primary neurons from E16 mouse at DIV10 were treated with indicated inhibitors for 48 hr. Conditioned medium (CM) and cell lysates were analyzed by immunoblot analysis with antibodies indicated below the panels.

(G) Densitometric analysis of sNLG1 (black bar) and NLG1-ICD (white bar) in (F) (n = 4–6, mean ± SEM; ***p < 0.001 versus DMSO; $^{###}$p < 0.001 versus DAPT by Student's t test).

(H) Schematic depiction of NLG processing.

that ADAM10 and γ-secretase are responsible for the proteolytic processing of NLG1 in transfected fibroblasts.

To further examine the role of ADAM10 in the processing of endogenous NLG1, we treated rat primary neurons obtained from E18 pups with INCB3619, a known ADAM10/17 inhibitor (Witters et al., 2008). INCB3619 abolished the secretion of sNLG1 in a similar manner to that of sAPPα, the latter being generated by ADAM10 (IC_{50}: 1.6 μM) (Figures 3A and 3C). In contrast, treatment with INCB3420, a derivative of INCB3619 that harbors a moderate ADAM10/17 inhibitory activity but potently inhibits matrix metalloproteases (MMPs) (i.e., MMP2, MMP9, MMP12, and MMP15) (Zhou et al., 2006), decreased the NLG1 cleavage only at high concentrations (IC_{50}: >10 μM) (Figures 3B and 3C). In addition, INCB3420 did not affect the sNLG1 production by incubation of synaptoneurosome fraction of rat adult brain (Figure S2A). Moreover, other MMP-specific inhibitors with different chemical structures (MMP2, MMP3, MMP9, and MMP13 inhibitors) did not affect the sNLG1

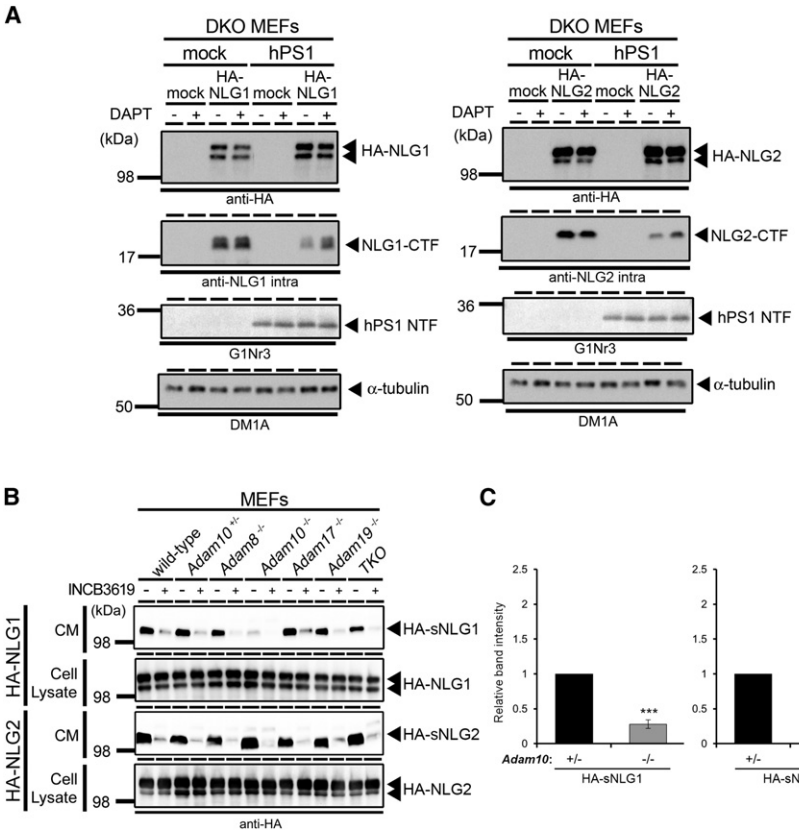

Figure 2. Proteolytic Processing of NLG1 in Presenilin or ADAM Knockout Cells

(A and B) Immunoblot analysis of HA-NLG1 or HA-NLG2 overexpressed in MEFs obtained from PS1/PS2 DKO (A) or ADAM KO (B) mice. Twenty-four hours after treatment of indicated compounds (i.e., 10 μM of DAPT in A, 10 μM of INCB3619 in B), CM and cell lysates were analyzed using antibodies indicated below the panels. Genotypes of ADAM knockout cells were indicated above the lanes. TKO denotes cells derived from *Adam9*$^{-/-}$; *Adam12*$^{-/-}$;*Adam15*$^{-/-}$ triple knockout mice.

(C) Densitometric analysis of HA-sNLG1 and HA-sNLG2 in *Adam10*$^{+/-}$ and *Adam10*$^{-/-}$ cells (B) (n = 4, mean ± SEM; ***p < 0.001 versus heterozygous cells [black bar] by Student's t test).

production or decreased only at high concentrations from rat primary neurons, supporting the specific role of ADAM proteases in NLG1 shedding in primary neurons (Figures 3B and 3D). We then examined the effect of genetic ablation of *Adam10* in mouse neuroblastoma neuro2a cells (Figures 3E and 3F) as well as in primary neurons from P1 *Adam10*$^{flox/flox}$ mice (Yoda et al., 2011) (Figures 3G and 3H) by siRNA transfection and overexpression of Cre recombinase, respectively. Inhibition of NLG1 shedding, along with impairment of sAPPα generation as previously described (Jorissen et al., 2010; Kuhn et al., 2010), and accumulation of NLG1-FL were observed both in *Adam10* knockdown neuro2a cells and *Adam10* knockout neurons. Moreover, overexpression of ADAM10 in mouse primary neurons increased the production of sNLG1 (Figure S2B). Lastly, to demonstrate the physiological significance of ADAM10 in NLG1 processing in vivo, we incubated the brain microsome from postnatal day (P) 18 neuron-specific conditional ADAM10 knockout mice (*Adam10*$^{flox/flox}$; *CamKII-Cre*) (Figure 3I). Notably, the levels of NLG1-FL were increased in the microsome fractions from brains of *Adam10* conditional knockout mice, whereas sNLG1 production was significantly decreased (Figures 3J and 3K). Taken together, we concluded that the major physiological sheddase of NLG1 in brain is ADAM10.

We next examined the proteolytic processing of NLG1 at the ectodomain in more detail. According to the molecular weight of the CTF, the stalk region of NLG1 is predicted as the candidate cleavage site for shedding. To obtain further precise information on the location and characteristics of the cleavage site, we analyzed mutant forms of NLG1 overexpressed in COS-1 cells (Figure 4A). Recombinant NLG1-FL was sequentially cleaved similarly to the endogenous NLG1-FL in primary neurons, whereas NLG1-ICD was not observed (Figures 4B and 4C). To identify the extracellular cleavage site of NLG1, we have systematically generated a series of alanine substitutions around the juxtamembrane stalk region, at sites consistent with the molecular weight of sNLG1 and NLG1-CTF: K^{674}QDD/AAAA, P^{678}KQQ/AAAA, P^{682}SPF/AAAA, S^{686}VDQ/AAAA, R^{690}DYS/AAAA, and T^{694}E/AA (Figure 4A). Among these mutants, generation of sNLG1 was significantly decreased in the PKQQ/AAAA mutant, whereas the level of mutant FL protein was increased (Figures 4D and 4E). The observation that overexpressed PKQQ/AAAA mutant NLG1 accumulated at dendritic spines in rat primary neurons similarly to wild-type (WT) NLG1 and showed spinogenic effects supported the view that introduction of PKQQ/AAAA mutation did not affect the trafficking of NLG1 (see Figure 8C). In contrast, alanine substitutions at regions proximal to the membrane caused an augmentation of NLG1 shedding. Intriguingly, the levels of sNLG1 were significantly increased in the PSPF/AAAA and SVDQ/AAAA mutants, whereas the corresponding FL proteins were decreased, suggesting that the region from Pro^{682} to Gln^{689} negatively regulates the NLG1 shedding. These data suggest that the region between Pro^{678} to Gln^{681} is critical for the sNLG1 production.

We then overexpressed NLG1-ΔE, a recombinant polypeptide corresponding to NLG-CTF starting from residue Val^{682} fused with a signal peptide (Figure 4A). The levels of NLG1-ΔE were increased by DAPT treatment, indicating that NLG1-ΔE was processed by γ-secretase (Figure 4F). However, NLG1-ICD was again undetectable in lysates of transfected cells. Indeed, recombinant NLG1-ICD, which corresponds to the predicted γ-secretase product starting at an intramembranous residue Val^{717}, was detected only after proteasome inhibitor treatment (Figure 4G), suggesting that NLG1-ICD is highly labile to proteasomal degradation. In fact, the immunostaining of NLG1-ICD

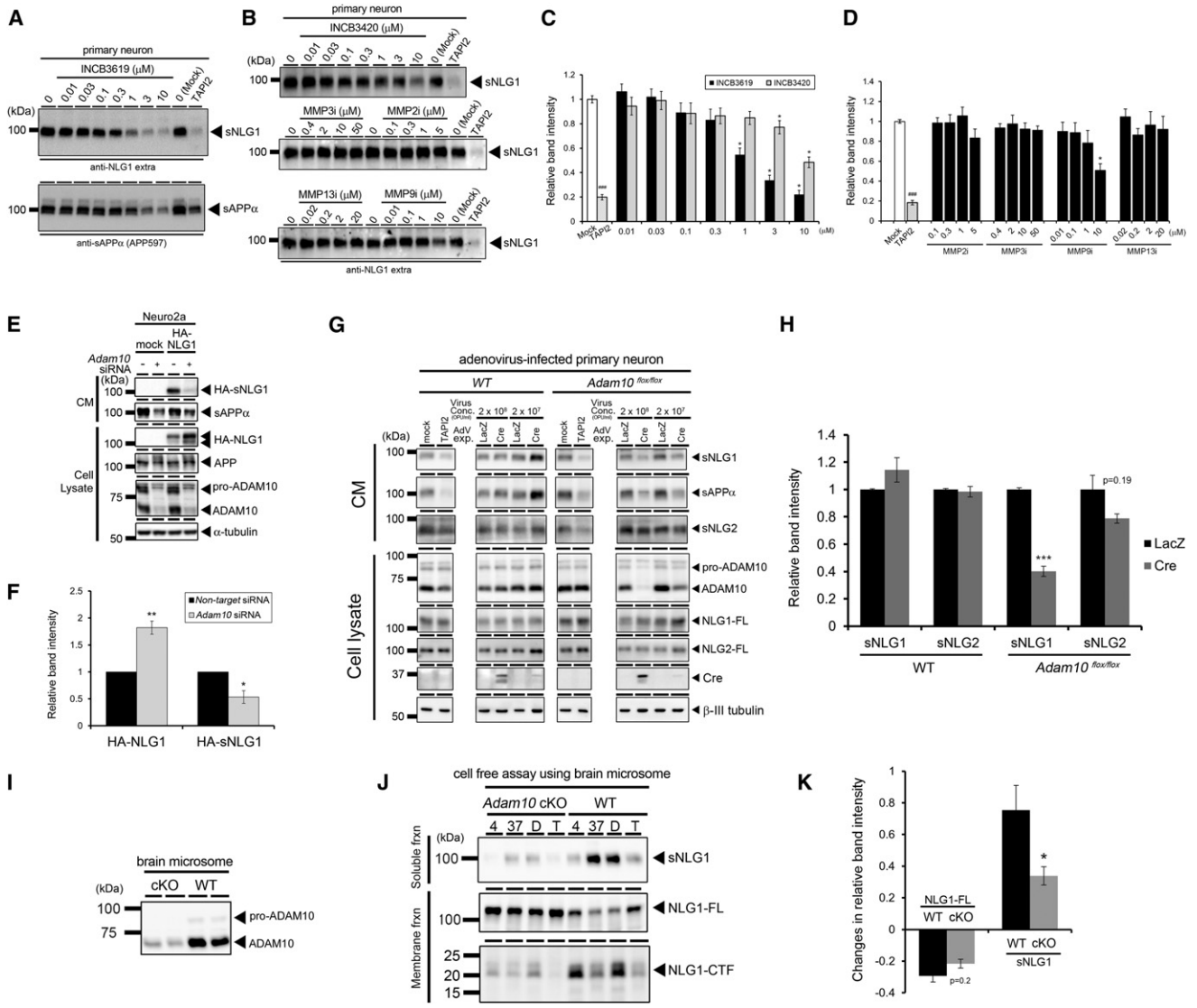

Figure 3. Pharmacological and Genetic Analyses of NLG1 Shedding in Neurons

(A and B) Immunoblot analysis of CM of rat primary neurons obtained from E17–E18 pups treated with ADAM (A) or MMP (B) inhibitors at DIV4. CM was collected at DIV6. Used compounds and concentration are shown above the lanes.

(C and D) Densitometric analysis of sNLG1 from neurons treated with ADAM (C) or MMP (D) inhibitors (n = 4–8, mean ± SEM; $^{###}p < 0.001$ versus mock by Student's t test; $^{*}p < 0.05$ versus mock by one-way ANOVA followed by Dunnett's post test).

(E) Immunoblot analysis of overexpressed HA-NLG1 in neuro2a cells cotransfected with siRNA duplex for nontarget or *Adam10*. CM and cell lysates were analyzed by immunoblotting using anti-HA for HA-NLG1, APP597 for endogenous APP, and anti-ADAM10 and DM1A for α-tubulin.

(F) Densitometric analysis of HA-NLG1 and HA-sNLG1 in (E) (n = 4, mean ± SEM; $^{*}p < 0.05$, $^{**}p < 0.01$ versus nontarget siRNA by Student's t test).

(G) Immunoblot analysis of mouse primary neurons infected with recombinant adenoviruses. Neurons were obtained from wild-type or *Adam10*$^{flox/flox}$ mouse at P1 and infected at DIV4 and replaced with fresh medium at DIV6. Samples were obtained at DIV8 and subjected to immunoblot analysis.

(H) Densitometric analysis of sNLG1 and sNLG2 in (G) (n = 3–6, mean ± SEM; $^{***}p < 0.001$ versus lacZ-infected cells by Student's t test).

(I) Immunoblot analysis of brain microsomes obtained from *Adam10*$^{flox/flox}$; *CamKII-Cre* (cKO) and *Adam10*$^{flox/flox}$ (WT) mice at P18.

(J) Cell-free assay of brain microsomes from cKO and WT mice. After incubation, samples were centrifuged to separate soluble and membrane fractions and then subjected to immunoblot analysis.

(K) Relative changes in the levels of NLG1-FL and sNLG1 in (J) compared with that at 4 degrees (n = 3, mean ± SEM; $^{*}p < 0.05$ versus WT by Student's t test).

was relatively weak and predominantly detected in neuronal nuclei and somata, whereas NLG1-FL, as well as the other mutants, was localized to the somatodendritic compartments in transfected primary neurons (Figure S3). We further examined the significance of the PDZ-binding motif located at the C terminus of NLG1 and found that deletion of this motif did not impact on the shedding as well as the γ-secretase-mediated cleavage (Figures 4A, 4B, 4C, and 4F). Collectively, these data

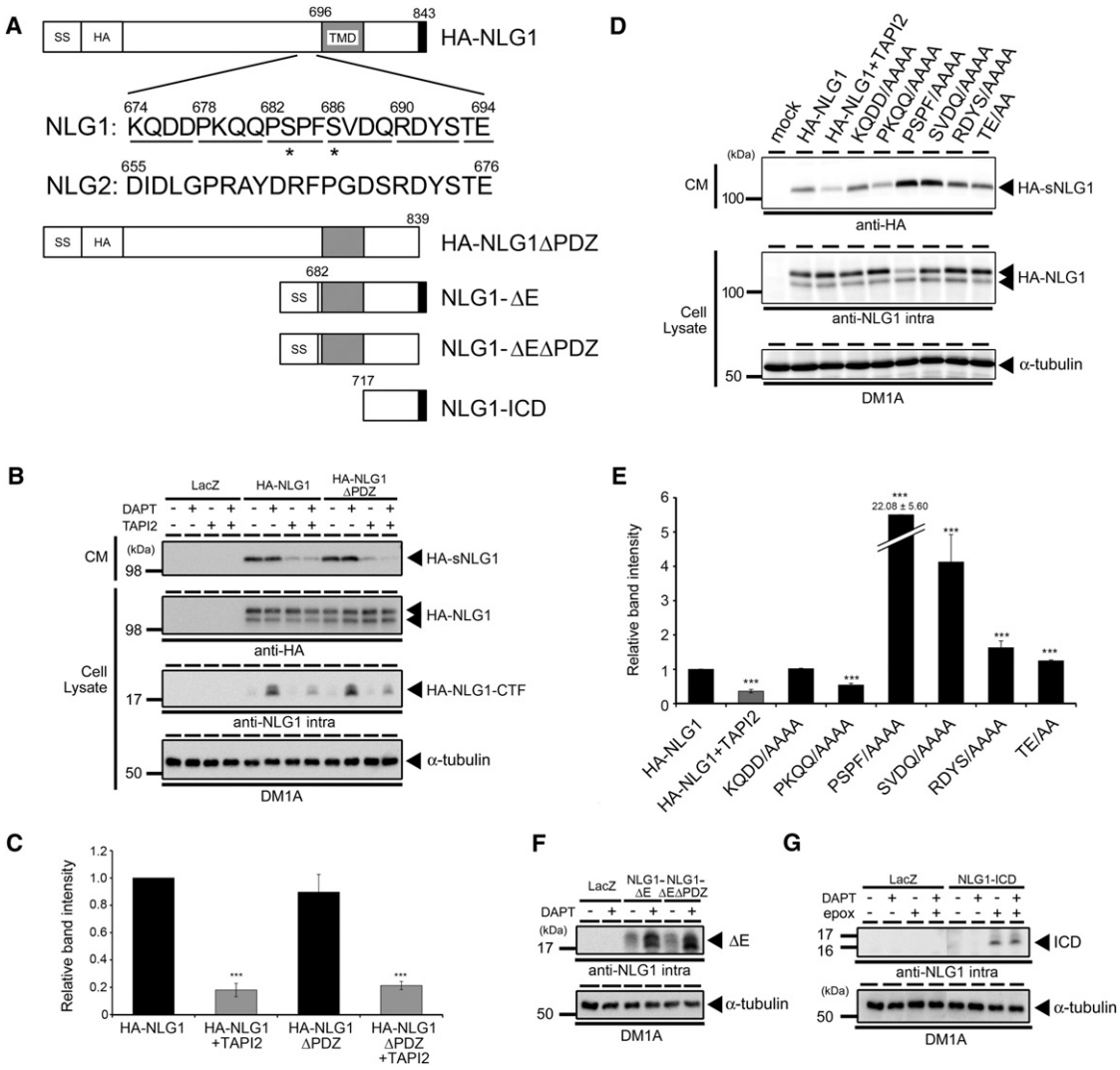

Figure 4. Proteolytic Processing of Mutant Forms of NLG1 at the Predicted Cleavage Site in COS-1 Cells

(A) Schematic depiction of mutant NLG1 constructs used in this study. Numbers represent corresponding amino acid residues in mouse NLG1. Transmembrane and PDZ-binding domains are indicated as gray and black boxes, respectively. Boxes with SS and HA represent signal sequence and inserted HA tag, respectively. Primary amino acid sequences of the stalk region of NLG1 and NLG2 are shown by single letter code. Locations of alanine substitution mutations in NLG1 were indicated by underbar. Asterisks represent *O*-glycosylation sites in the stalk region of NLG1.

(B–G) Immunoblot analysis of CM as well as lysates of COS cells expressing NLG1ΔPDZ (B), NLG1 with amino acid substitutions (D), NLG1-ΔE (F), or NLG1-ICD (G) treated with indicated compounds. Note that NLG1-ICD was detected only in epoxomicin (epox)-treated COS cells. Densitometric analysis of secreted HA-sNLG1 standardized by HA-NLG1 expression of lysates in (E) and (D) were shown in (C) and (E), respectively (n = 3, mean ± SEM; ***$p < 0.001$ versus HA-NLG1 by Student's t test).

support the notion that NLG1 is sequentially cleaved by ADAM10 and γ-secretase to release sNLG1 and a highly labile NLG1-ICD.

Neuronal Activity and Ligand Binding Upregulate NLG1 Processing

It has been shown that some γ-secretase substrates (e.g., APP, N-cadherin, and EphA4) undergo cleavage in an activity-dependent manner in neurons (Kamenetz et al., 2003; Marambaud et al., 2003; Reiss et al., 2005; Inoue et al., 2009). To investigate the effect of synaptic activity on NLG1 processing, we treated rat primary neuronal culture at day in vitro (DIV) 11 with a set of compounds. Fifteen minute treatments with glutamate or NMDA significantly increased the sNLG1 level in the conditioned media, which was abolished by addition of NMDA receptor antagonists (i.e., D-AP5 and MK-801) (Figures 5A and 5B). Intriguingly, pretreatment with MK-801 (Figures 5C and 5D), an open-channel blocker of NMDA receptor (Huettner and Bean, 1988), completely inhibited the NLG1 shedding induced by glutamate, suggesting that the physiological activation of functional NMDA receptors is sufficient for the generation of sNLG1 at the glutamatergic synapses. To examine whether the shedding regulates the cell surface level of NLG1, we performed

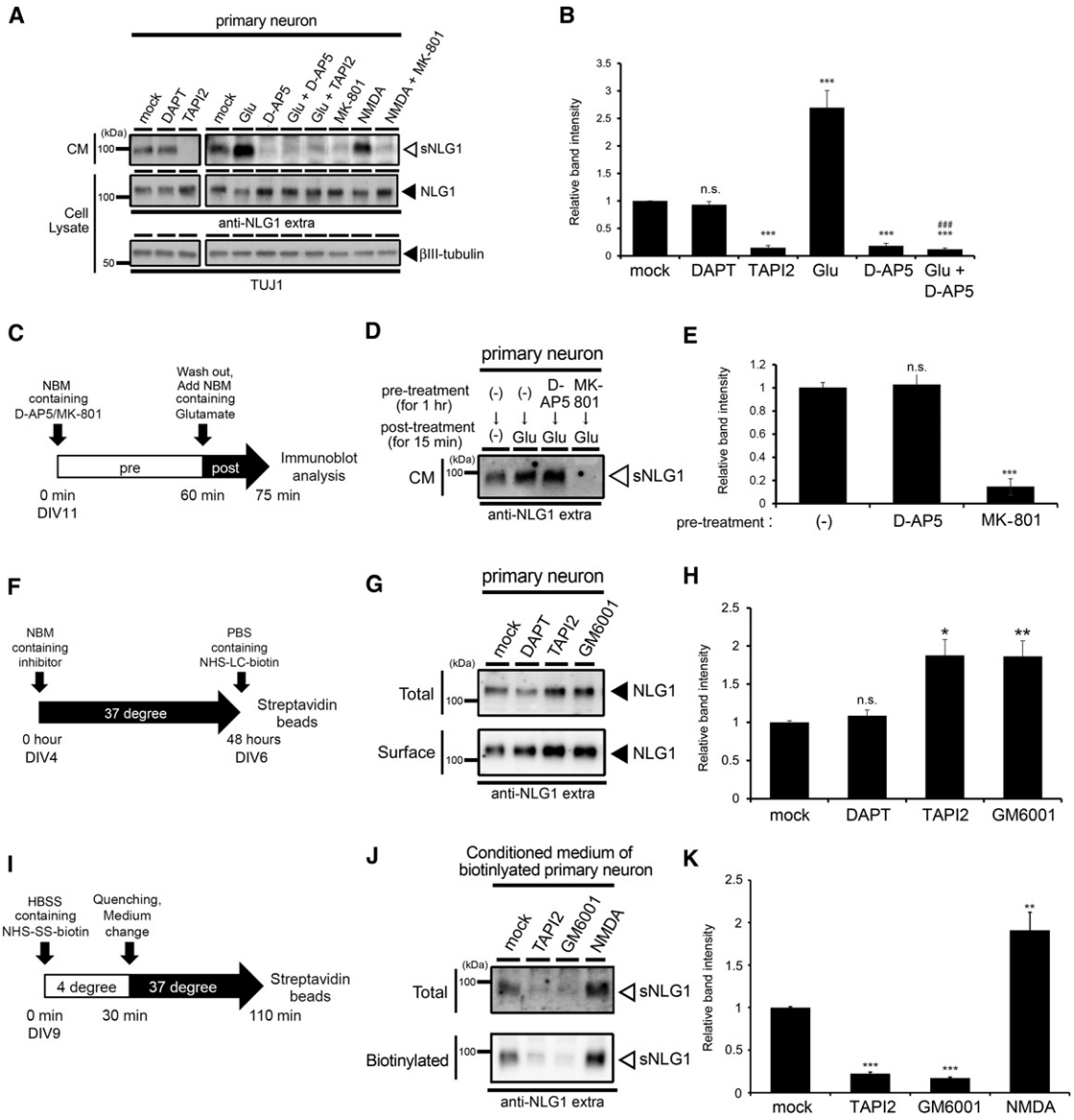

Figure 5. Activity-Dependent Shedding of NLG1 in Primary Neurons

(A) Primary neurons from E18 rat cortex were treated with indicated compounds at DIV11 for 15 min. CM as well as cell lysates were analyzed by immunoblotting using antibodies indicated below the panels.

(B) Densitometric analysis of the amounts of sNLG1 secreted from rat primary neurons treated as in (A). Statistical analysis was carried out by Student's t test (n = 5–9, mean ± SEM, ***$p < 0.001$ versus mock; $^{###}p < 0.001$ versus Glu).

(C–E) Production of sNLG1 from rat primary neurons from E17–E18 pups pretreated with NMDAR antagonists at DIV11 (C). Representative result of immunoblot analysis of CM is shown in (D). Noncompetitive NMDAR antagonist, MK-801, totally abolished the production of sNLG1. NBM indicates Neurobasal medium. Densitometric analysis of sNLG1 is shown in (E) (n = 3, mean ± SEM; ***$p < 0.001$ versus (–) by Student's t test).

(F–H) Surface protein levels were examined by the surface biotinylation technique in rat primary neurons obtained from E17–E18 pups at DIV6 (F). Representative result of immunoblot analysis is shown in (G). TAPI2 or GM6001 treatment from DIV4 to DIV6 caused a significant accumulation of total as well as cell surface NLG1. Densitometric analysis of sNLG1 is shown in (H) (n = 4, mean ± SEM; *$p < 0.05$; **$p < 0.01$ versus by Student's t test).

(I–K) Detection of de novo secretion of biotinylated sNLG1 from DIV9 rat primary neurons from E17–E18 pups (I). Representative result of immunoblot analysis is shown in (J). Densitometric analysis of sNLG1 is shown in (K) (n = 3–5, mean ± SEM; **$p < 0.01$; ***$p < 0.001$ versus mock by Student's t test).

a cell surface biotinylation experiment in rat primary neurons (Figure 5F). Treatment with TAPI2 or GM6001 significantly increased the surface levels of NLG1 (Figures 5G and 5H). Moreover, secretion of biotinylated sNLG1 was detected in the conditioned media of labeled primary neurons (Figures 5I, 5J, and 5K). Notably, increased sNLG1 by NMDA treatment also was biotinylated, suggesting that the proteolytic processing of NLG1 occurs at the cell surface and regulates the levels of cell surface

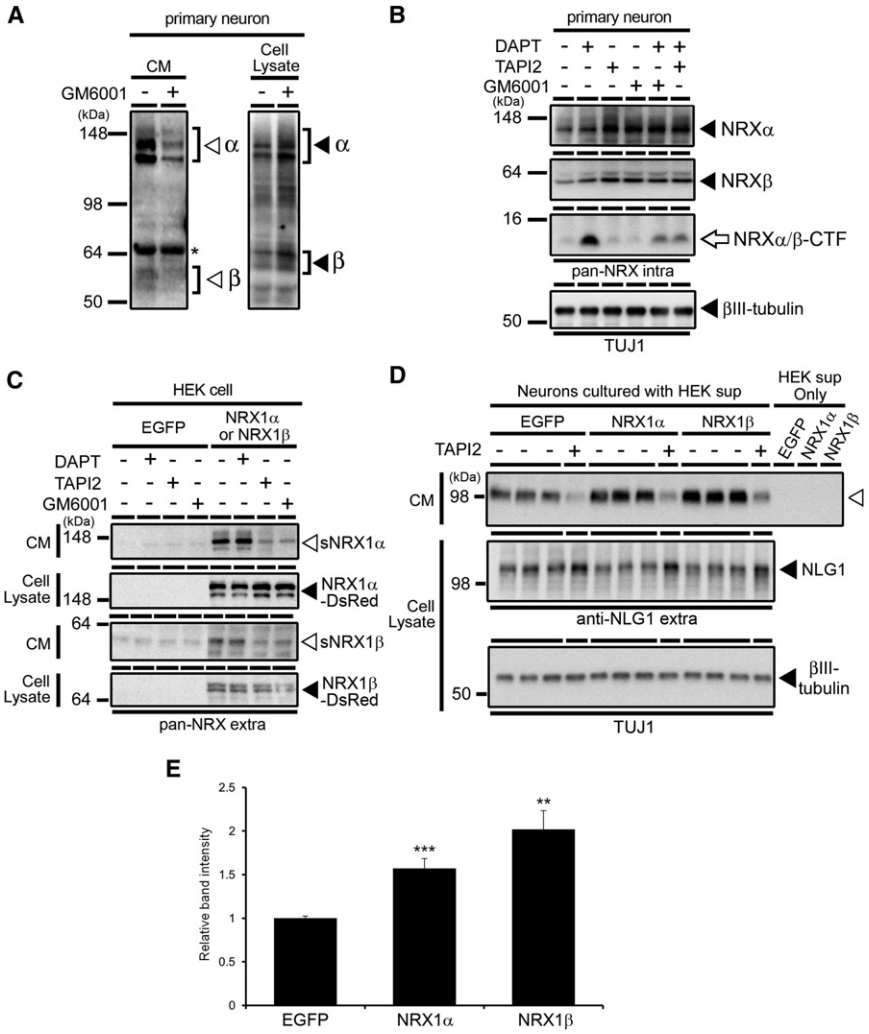

Figure 6. Increased Shedding of NLG1 by Soluble NRXs Derived by Proteolytic Processing

(A and B) Immunoblot analysis of serum-free CM as well as cell lysates of primary neurons with indicated compounds. Antibody against extracellular (A) or intracellular (B) domain of NRX was used.

(C) Metalloprotease-dependent secretion of recombinant soluble NRXs from HEK293T stably expressing NRX1α-dsRed or NRX1β-dsRed.

(D) DIV11 primary neurons from E18 rat were cultured for 24 hr in the presence of conditioned media derived from HEK293T stably expressing NRX1α or 1β, which was analyzed in (C). The levels of sNLG1 (white arrowhead) and NLG1-FL (black arrowhead) were analyzed by immunoblotting.

(E) Densitometric analysis of sNLG1 in (D) (n = 5–6, mean ± SEM; **p < 0.01; ***p < 0.001 versus EGFP by Student's t test).

NLG1. Taken together with the results of synaptoneurosome incubation (Figure 1D), these data indicate that glutamatergic synaptic transmission through NMDA receptor activation modulates the levels of NLG1 at the synaptic membrane.

It has been shown that several γ-secretase substrates are cleaved upon binding with cognate membrane-tethered or soluble ligands, e.g., Delta/Jagged for Notch (Mumm et al., 2000), Hyaluronan for CD44 (Sugahara et al., 2003), BDNF for p75 (Kenchappa et al., 2006), and VEGF-A for VEGF receptor (Swendeman et al., 2008). Recently, it was reported that NRXs undergo proteolytic processing, which is augmented by glutamate treatment (Bot et al., 2011; Saura et al., 2011). We also observed the metalloprotease-dependent production of soluble forms of endogenous NRXs in rat primary neurons (Figure 6A). Treatment with TAPI2 or GM6001 caused the accumulation of NRX-FL and inhibited the accumulation of NRX-CTF, which was detected upon DAPT treatment (Figure 6B). These data indicate that NRXs also are sequentially cleaved by metalloprotease and γ-secretase in primary neurons. To investigate whether the binding of NRX regulates the production of sNLG1, we coincubated primary neurons with the conditioned media of HEK293T cells expressing NRX1α or NRX1β, which contained soluble forms of the NRXs (Figure 6C). Accumulation of NRX1β immunoreactivity at endogenous NLG1 puncta was observed in rat primary neurons treated with the HEK293T conditioned media containing sNRX1β, suggesting that recombinant sNRX1β is capable of interacting with NLG1 at synapses (Figure S4). Intriguingly, release of sNLG1 from neurons was significantly increased by addition of the soluble NRX-containing media (Figures 6D and 6E). This result indicates that ligand binding at the cell surface regulates the shedding of NLG1.

We also analyzed the activity-dependent NLG1 processing in vivo. Pilocarpine treatment induces glutamate-mediated synaptic activation, resulting in status epilepticus associated with synapse remodeling (Isokawa, 1998; Kurz et al., 2008). In agreement with the previous reports (Kamenetz et al., 2003), APP processing was promoted in the brains of 8-week-old epileptic mice (Figure 7A). Moreover, the level of sNLG1 was significantly increased, whereas that of the membrane-associated NLG1-FL was decreased, suggesting that NLG1 shedding was augmented in brains by pilocarpine-induced seizures (Figure 7B). Taken together, these data suggest that NLG1 processing is modulated by the excitatory activity in vivo as well as in vitro.

The Effect of NLG1 Processing on the Spine Density

To analyze the functional impact of NLG1 processing on its spinogenic activity, we overexpressed NLG1 and its derivatives in dentate granule cells of the organotypic hippocampal slice culture obtained from P6 rat, in which local-circuit synaptic interactions are preserved. Overexpression of NLG1-FL significantly increased the spine density at the apical dendrites of granule cells. However, NLG2-FL failed to induce spines, suggesting that NLG1 specifically increased the spine density at

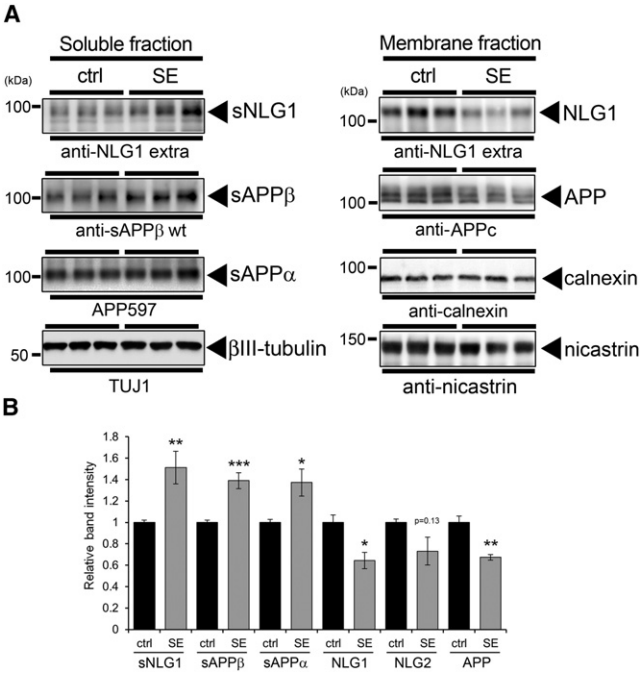

Figure 7. Status Epilepticus Induced by Pilocarpine Promoted the Shedding of NLG1 In Vivo

(A) Immunoblot analysis of TS soluble (soluble fraction, left) and insoluble (membrane fraction, right) of cortices from 8-week-old mice with status epilepticus (SE) 1 hr after the injection of pilocarpine. Mice injected with saline were used as control (ctrl). NLG1, APP, and their derivatives were probed with relevant antibodies. βIII-tubulin, calnexin, and nicastrin were used as loading controls for each fraction, respectively. A representative set of immunoblot data is shown.

(B) Densitometric analysis of immunoblots. Protein levels in SE brain were standardized by those in the control brains. Statistical analysis was carried out by Student's t test (n = 5, mean ± SEM, *p < 0.05; **p < 0.01, ***p < 0.001 versus ctrl).

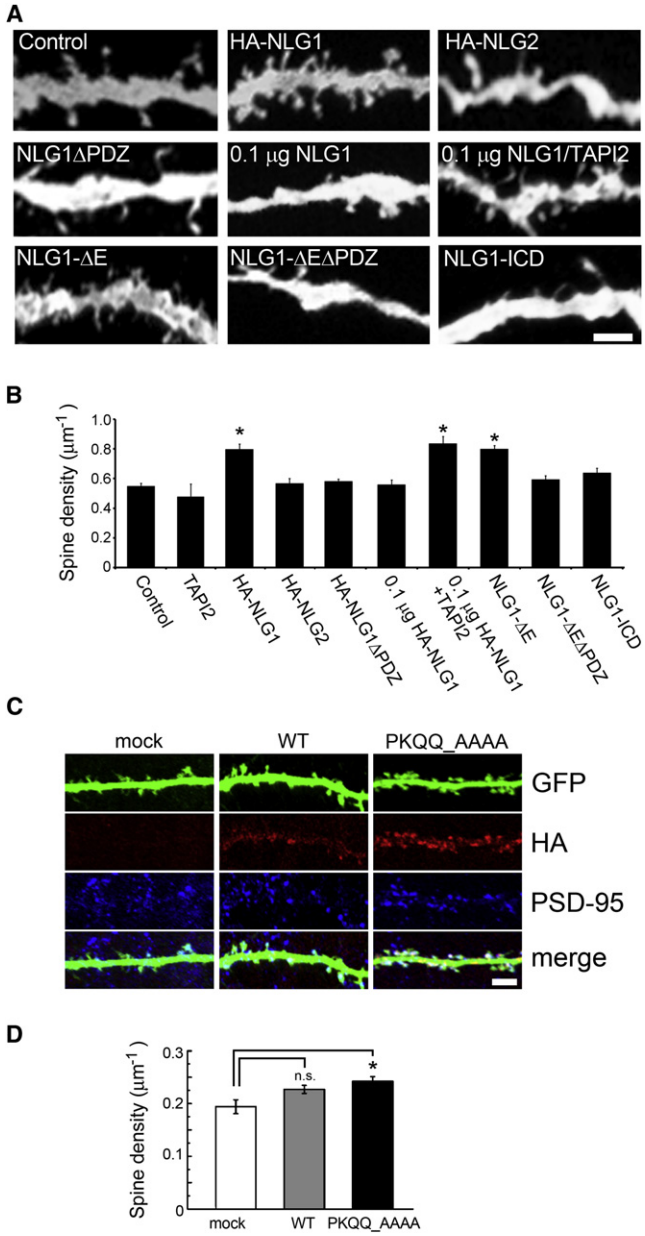

Figure 8. Effect of Truncated NLG1 on Spine Formation

(A) Representative confocal images of apical dendrites visualized by GFP in rat hippocampal slice cultures prepared from P6 rats transfected with GFP with NLG1 constructs. We used 1 μg of plasmids for recombinant proteins unless the amount is indicated. White bar represents 1 μm.

(B) Quantification of the spine density of neurons in the indicated conditions. Statistical analysis was carried out by Dunnett's multiple comparison test (n = 6–35, mean ± SEM, *p < 0.01 versus mock).

(C) Representative confocal images of immunostained dendrites in rat hippocampal primary neurons obtained from E17–E18 pups transfected with GFP and WT or PKQQ_AAAA mutant NLG1. Transfection into rat primary neurons was performed at DIV6 and fixed at DIV20. White bar represents 5 μm.

(D) Quantification of the spine density of neurons under the indicated conditions. Statistical analysis was carried out by Dunnett's multiple comparison test (n = 14 [mock], 55 [WT], and 42 [PKQQ_AAAA]). Mean ± SEM, *p < 0.05 versus mock.

glutamatergic synapses as previously described (Figure 8A) (Scheiffele et al., 2000; Graf et al., 2004). Overexpression of NLG1ΔPDZ that lacks the C terminus failed to increase the spine number, suggesting that the spinogenic effect of NLG1 is dependent on the PDZ-binding motif in rat dentate granule cells. Reduction in the amount of transfected NLG1 cDNA led to loss of the spinogenic effect of NLG1 (see 0.1 μg HA-NLG1, Figures 8A and 8B), indicating that the protein level of NLG1 is critical to the de novo formation of the dendritic spine (Figure 8B). Notably, TAPI2 treatment of cultures transfected with reduced amount of HA-NLG1 cDNA (0.1 μg/ml) recovered the incremental effect on spine density to a level comparable to that in cells transfected with 1.0 μg/μl of HA-NLG1. Thus, we reasoned that ectodomain shedding negatively regulates the spinogenic effect of NLG1 in hippocampal granule cells. Next, we analyzed the effects of fragment forms of NLG1 corresponding to its proteolytic products (i.e., NLG1-ΔE and NLG1-ICD) on the spine density (Figure 8A). Unexpectedly, NLG1-ΔE increased the spine density at a similar level to NLG1-FL, suggesting that the NLG1-CTF lacking the ectodomain retains the spinogenic effect. However, NLG1-ICD failed to increase the spine density. Thus, the function of membrane-tethered form of NLG1-ICD (aka,

NLG1-ΔE or NLG1-CTF) was abolished by liberation from the membrane by the γ-secretase cleavage and subsequent degradation. Finally, to directly test whether NLG1 shedding modulates the spinogenic function, we analyzed the dendritic spines of transfected rat hippocampal primary neurons obtained from E18 pups (Figure 8C). We transfected wild-type or PKQQ/AAAA mutant NLG1 together with green fluorescent protein (GFP) into primary neurons at DIV6 and fixed them at DIV20. The numbers of spines in neurons expressing wild-type NLG1 showed an increased trend compared to those in mock-transfected neurons, but not with a statistical significance. However, the spine density was significantly increased in neurons transfected with the mutant NLG1 (Figure 8D), suggesting that cleavage-deficient mutation enhanced the NLG1 function in primary neurons. Taken together, our results indicate that the sequential processing of NLG1 negatively regulates the spinogenic activity.

DISCUSSION

Sequential Proteolytic Processing of NLG1 by ADAM10 and γ-Secretase

To date, all known γ-secretase substrates are shown to be first shed at the extracellular domain to generate a soluble ectodomain as well as a membrane-tethered CTF. ADAM10 is a well-characterized physiological sheddase for a number of γ-secretase substrates (e.g., APP, cadherin, and Notch) (Reiss et al., 2005; Jorissen et al., 2010; Kuhn et al., 2010). Both γ-secretase and ADAM10 have been implicated in the regulation of neural stem cell number by modulation of Notch signaling in the developing CNS (Jorissen et al., 2010). Recently, it was shown that metalloprotease and γ-secretase-mediated cleavage in mature neurons regulates the synaptic function (Rivera et al., 2010; Restituito et al., 2011). Here we systematically analyzed the processing of NLG1 by pharmacological and genetic approaches. Using specific inhibitors and Cre-mediated gene excision, we found that ADAM10 is responsible for NLG1 shedding and that C-terminal stub of NLG1 is subsequently cleaved by γ-secretase (Figure 1F). Notably, significant reduction in the sNLG1 production was similarly observed in two distinct lines of *Adam10*$^{flox/flox}$ mice (i.e., exon 1 floxed mice for in vitro Cre-mediated gene excision in primary neurons and exon 2 floxed mice for cKO mice), indicating that ADAM10 is a major sheddase for NLG1 in vivo in brains. In addition, *Adam10*-dependent sNLG1 production and NLG1 accumulation were observed in primary neurons as well as in adult mouse brains, suggesting that NLG1 is shed by ADAM10 at both developmental and mature stages in neurons. Our data unequivocally indicate that the cell surface level of NLG1 is regulated by ADAM10/γ-secretase-mediated sequential processing, which may in turn negatively modulate its spinogenic activity.

It is noteworthy that ADAM10 prefers Leu, Phe, Tyr, and Gln at P1′ position for cleavage (Caescu et al., 2009), although no consensus cleavage sequence has been reported. Our observation that shedding of NLG1 was inhibited in PKQQ/AAAA mutant suggests that the Gln^{680} or Gln^{681} at the stalk region of NLG1 is the candidate cleavage site for ADAM10-mediated shedding. Unexpectedly, we found that NLG2 was not a suitable substrate for ADAMs so far examined. This is consistent with the previous results that ADAM10 is localized at the excitatory postsynapses at which NLG1 is present (Marcello et al., 2007), whereas NLG2 resides in the GABAergic postsynapses (Graf et al., 2004). Indeed, primary amino acid sequence of the stalk region of NLG2 is totally different from that of NLG1 (Figure 3A). Thus, other metalloprotease(s) present in the inhibitory synapse should be responsible for NLG2 shedding. Intriguingly, the expression levels of NLG1, but not NLG2, was significantly increased in the brains of ADAM10 transgenic mice, suggesting a specific functional correlation between NLG1 and ADAM10 (Prinzen et al., 2009). Identification of the responsible proteases and relevant auxiliary components at different types of synapses would provide important information on the proteolytic control of neuronal adhesion molecules.

Physiological Significance of the Activity-Dependent Processing of NLG1

The level of NLG1 in neurons has been shown to regulate the number, ratio of NMDA/AMPA receptors, and electrophysiological functions of the excitatory synapses in vitro and in vivo (Song et al., 1999; Chih et al., 2006; Varoqueaux et al., 2006; Chubykin et al., 2007). Here, we show that NLG1 is cleaved in a neuronal activity-dependent manner, resulting in a loss of its spinogenic function. Moreover, pretreatment with MK-801 completely abolished the processing of NLG1 induced by glutamate, suggesting that the NLG1 level is homeostatically controlled by the excitatory synaptic, but not extrasynaptic, transmission. Increased shedding of NLG1 was also observed in pilocarpine-treated mice. Interestingly, profound decreases in the density, as well as alterations in shape and size, of dendritic spines by aberrant Ca^{2+} signaling have been observed in epileptic mouse models (Isokawa, 1998; Kochan et al., 2000; Kurz, et al., 2008). Aberrant Ca^{2+} signaling also affects ADAM10 activity via calmodulin kinase as well as calcineurin (Nagano et al., 2004; Kohutek et al., 2009). These results support the idea that NLG1 processing is involved in the remodeling of dendritic spines at glutamatergic synapses in vivo. We also found that soluble NRX treatment augments the NLG1 shedding. In this regard, the activity-dependent proteolytic cleavage of NRX at the presynapse (Bot et al., 2011; Saura et al., 2011) may be functionally linked to the processing of NLG. It has been reported that Fc-fused recombinant NRX extracellular domain inhibited the synaptogenic activity of NLG (Scheiffele et al., 2000; Levinson et al., 2005); it is possible that soluble NRX functions as a negative regulator of NLG1 via induction of shedding. Ligand-induced shedding has been reported in several γ-secretase substrates (Mumm et al., 2000; Sugahara et al., 2003; Kenchappa et al., 2006; Findley et al., 2007) too, although the molecular mechanisms whereby the ligands activate the processing remain unknown. Ligand/receptor complex formation has been shown to increase the ADAM activity in the ephrin/Eph receptor system (Janes et al., 2009). In the case of Notch, "pulling" movement induced by the endocytosis of bound ligand is thought to cause a structural change leading to cleavage (Gordon et al., 2007). Notably, mucin-like *O*-linked glycosylation, which might create steric hindrance against ADAM10, was identified in the juxtamembranous stalk region of NLG1 (i.e., Ser^{683} and Ser^{686}, respectively; Hoffman et al., 2004). We also have found that

amino acid substitutions including the *O*-glycosylation sites (i.e., PSPF/AAAA and SVDQ/AAAA mutants) increased the shedding of NLG1 (Figure 4C). Thus, it is possible that the binding of soluble NRX induces structural changes in the stalk region of NLG1 in a way to expose the cleavage site and/or activate the ADAM10 activity. Further studies on the mechanism of ADAM10 activation as well as structural analyses of the cleavage site would clarify the mechanism of NLG1 shedding.

What, then, is the physiological function of the NLG1 fragments? Extracellular domain of NLG1 is sufficient for binding its ligands (Ichtchenko et al., 1995). Intriguingly, soluble form of NLG1 has been shown to inhibit the synaptogenic effect of TSP1 in immature neurons (Xu et al., 2010). Moreover, clustering of NRXs by recombinant NLG1 extracellular domain mediated the assembly of presynaptic terminals (Dean et al., 2003), raising the possibility that sNLG1 may bind to soluble as well as membrane-tethered forms of ligands and modulate their functions. Unexpectedly, however, overexpression of NLG1-ΔE that lacks the extracellular domain retained the capacity to induce dendritic spines in granule cells. Our observation is consistent with the previous data showing that the conserved cytoplasmic domain, rather than NRX binding, is necessary and sufficient for the induction of dendritic spines by NLG1 in transfected neurons (Ko et al., 2009; Shipman et al., 2011). Importantly, however, overexpression of NLG1-ICD, which retains the intact intracellular domain, failed to increase the spine numbers. Moreover, NLG1-ICD was highly labile and degraded by proteasomal activity. These data indicate that the membrane tethering as well as the stability of the cytoplasmic domain of NLG1 is critical to the spinogenic activity. This is distinct from the activation of the "conventional" γ-secretase substrates, e.g., Notch, by γ-cleavage, although there also are several examples of negative regulation of the functions of γ-secretase substrates by cleavage, e.g., ephrin-B1 and DCC (Tomita et al., 2006; Parent et al., 2005).

Taken together, our present results provide compelling evidence that proteolytic processing is a molecular mechanism regulating the NLG1 levels as well as its spinogenic function. Further functional analysis would be required to determine whether spines modulated by NLG1 shedding are functional. However, previous results showing that changes in spines by overexpression or knockdown of NLG1 correlated with synaptic transmission (Chih et al., 2006; Levinson et al., 2005; Chubykin et al., 2007) may support our view that the proteolytic cleavage by ADAM10 and γ-secretase downregulates the cell-surface levels of NLG1, which in turn negatively affects the synaptogenic function. Considering the recent implication of aberrant levels of expression of NLGs or NRXs in ASD, it is tempting to speculate that alterations in the proteolytic processing of NLG1 may also be involved in the etiology of the neurodevelopmental abnormalities.

EXPERIMENTAL PROCEDURES

Chemicals, Immunological Methods, Animals, Plasmids, Cell Culture, Transfection, Recombinant Virus Infection, and RNA Interference

All experimental procedures were performed in accordance with the guidelines for animal experiments of the University of Tokyo. Primary neuron culture, immunoblot analyses, and immunocytochemistry experiments were performed as previously described with some modifications (Tomita et al., 1998; Fukumoto et al., 1999). For in vitro Cre-mediated *Adam10* ablation, primary cortical neurons were obtained from E16 pups of *Adam10*$^{flox/flox}$ mice, in which the first exon was floxed (Yoda et al., 2011). For analysis of neuron-specific conditional *Adam10* knockout mice, brains of P18 exon 2 floxed *Adam10*$^{flox/flox}$ mice (Jorissen et al., 2010) crossed with CamKII-Cre mice (J.P. and P.S., unpublished data) were homogenized to obtain microsome fractions. Other animals were obtained from Japan-SLC. See Supplemental Experimental Procedures for details.

Mouse Model of Status Epileptics by Pilocarpine Treatment

Male 8-week-old BALB/C mice were injected with scopolamine methylnitrate (Tokyo Chemical Industry) (1 mg/kg, intraperitoneally [i.p.]) to protect against peripheral autonomic effects caused by subsequent pilocarpine administration. Fifteen to thirty minutes later, mice were injected with pilocarpine-HCl (SIGMA) (330–380 mg/kg, i.p.) or saline (Otsuka), and then we scored the seizure intensity according to a previously described method (Patel et al., 1988). We defined status epilepticus (status epilepsy) as a continuous seizure lasting longer than 30 min. One hour after the injection of pilocarpine, mice were sacrificed to isolate the cerebrums. See Supplemental Experimental Procedures for details.

Analysis of Spinogenic Function of NLG1

Hippocampal slice cultures were prepared from P6 rats as previously described (Koyama et al., 2007). Granule cells in the cultured slices at DIV5 were transfected with the plasmids encoding NLG1 and its derivatives (1.0 μg/μl in HBSS) using the single-cell electroporation method (Nakahara et al., 2009). Transfection of mutant NLG1 in rat hippocampal primary neurons were performed at DIV6 and fixed at DIV20. See Supplemental Experimental Proceduresfor details.

SUPPLEMENTAL INFORMATION

Supplemental Information includes four figures and Supplemental Experimental Procedures and can be found with this article online at http://dx.doi.org/10.1016/j.neuron.2012.10.003.

ACKNOWLEDGMENTS

We thank Drs. C. Blobel (Hospital for Special Surgery, New York), R. Balice-Gordon (University of Pennsylvania), P. Scheiffele (University of Basel), B. De Strooper (VIB Leuven), K. Hozumi (Tokai University), F. Fahrenholtz (Johannes Gutenberg University Mainz), T. Kitamura (The University of Tokyo), and J. Takagi (Osaka University) for materials. We are also grateful to our laboratory members for helpful discussions and technical assistance. This work was supported by Grants-in-Aid for Young Scientists (S) from Japan Society for the Promotion of Science (JSPS) (for T.T.), Challenging Exploratory Research from JSPS (for T.T.), Scientific Research on Innovative Areas "Foundation of Synapse and Neurocircuit Pathology" from the Ministry of Education, Culture, Sports, Science, and Technology (MEXT) (for T.T. and T.I.), the Cell Science Research Foundation (for T.T.), Core Research for Evolutional Science and Technology of the Japan Science and Technology Agency (for Y.H., T.T., and T.I.), Japan, and the Deutsche Forschungsgemeinschaft SFB877 TP:A3 (for P.S.). K.S. is a research fellow of JSPS.

Accepted: October 2, 2012
Published: October 18, 2012

REFERENCES

Bai, G., and Pfaff, S.L. (2011). Protease regulation: the Yin and Yang of neural development and disease. Neuron *72*, 9–21.

Beel, A.J., and Sanders, C.R. (2008). Substrate specificity of γ-secretase and other intramembrane proteases. Cell. Mol. Life Sci. *65*, 1311–1334.

Blundell, J., Blaiss, C.A., Etherton, M.R., Espinosa, F., Tabuchi, K., Walz, C., Bolliger, M.F., Südhof, T.C., and Powell, C.M. (2010). Neuroligin-1 deletion

results in impaired spatial memory and increased repetitive behavior. J. Neurosci. *30*, 2115–2129.

Bot, N., Schweizer, C., Ben Halima, S., and Fraering, P.C. (2011). Processing of the synaptic cell adhesion molecule neurexin-3β by Alzheimer disease α- and γ-secretases. J. Biol. Chem. *286*, 2762–2773.

Bottos, A., Rissone, A., Bussolino, F., and Arese, M. (2011). Neurexins and neuroligins: synapses look out of the nervous system. Cell. Mol. Life Sci. *68*, 2655–2666.

Budreck, E.C., and Scheiffele, P. (2007). Neuroligin-3 is a neuronal adhesion protein at GABAergic and glutamatergic synapses. Eur. J. Neurosci. *26*, 1738–1748.

Caescu, C.I., Jeschke, G.R., and Turk, B.E. (2009). Active-site determinants of substrate recognition by the metalloproteinases TACE and ADAM10. Biochem. J. *424*, 79–88.

Chih, B., Gollan, L., and Scheiffele, P. (2006). Alternative splicing controls selective trans-synaptic interactions of the neuroligin-neurexin complex. Neuron *51*, 171–178.

Chubykin, A.A., Atasoy, D., Etherton, M.R., Brose, N., Kavalali, E.T., Gibson, J.R., and Südhof, T.C. (2007). Activity-dependent validation of excitatory versus inhibitory synapses by neuroligin-1 versus neuroligin-2. Neuron *54*, 919–931.

Comoletti, D., De Jaco, A., Jennings, L.L., Flynn, R.E., Gaietta, G., Tsigelny, I., Ellisman, M.H., and Taylor, P. (2004). The Arg451Cys-neuroligin-3 mutation associated with autism reveals a defect in protein processing. J. Neurosci. *24*, 4889–4893.

Dahlhaus, R., Hines, R.M., Eadie, B.D., Kannangara, T.S., Hines, D.J., Brown, C.E., Christie, B.R., and El-Husseini, A. (2010). Overexpression of the cell adhesion protein neuroligin-1 induces learning deficits and impairs synaptic plasticity by altering the ratio of excitation to inhibition in the hippocampus. Hippocampus *20*, 305–322.

Dalva, M.B., McClelland, A.C., and Kayser, M.S. (2007). Cell adhesion molecules: signalling functions at the synapse. Nat. Rev. Neurosci. *8*, 206–220.

Dean, C., Scholl, F.G., Choih, J., DeMaria, S., Berger, J., Isacoff, E., and Scheiffele, P. (2003). Neurexin mediates the assembly of presynaptic terminals. Nat. Neurosci. *6*, 708–716.

Findley, C.M., Cudmore, M.J., Ahmed, A., and Kontos, C.D. (2007). VEGF induces Tie2 shedding via a phosphoinositide 3-kinase/Akt dependent pathway to modulate Tie2 signaling. Arterioscler. Thromb. Vasc. Biol. *27*, 2619–2626.

Fukumoto, H., Tomita, T., Matsunaga, H., Ishibashi, Y., Saido, T.C., and Iwatsubo, T. (1999). Primary cultures of neuronal and non-neuronal rat brain cells secrete similar proportions of amyloid β peptides ending at Aβ40 and Aβ42. Neuroreport *10*, 2965–2969.

Glessner, J.T., Wang, K., Cai, G., Korvatska, O., Kim, C.E., Wood, S., Zhang, H., Estes, A., Brune, C.W., Bradfield, J.P., et al. (2009). Autism genome-wide copy number variation reveals ubiquitin and neuronal genes. Nature *459*, 569–573.

Gordon, W.R., Vardar-Ulu, D., Histen, G., Sanchez-Irizarry, C., Aster, J.C., and Blacklow, S.C. (2007). Structural basis for autoinhibition of Notch. Nat. Struct. Mol. Biol. *14*, 295–300.

Graf, E.R., Zhang, X., Jin, S.X., Linhoff, M.W., and Craig, A.M. (2004). Neurexins induce differentiation of GABA and glutamate postsynaptic specializations via neuroligins. Cell *119*, 1013–1026.

Hartmann, D., de Strooper, B., Serneels, L., Craessaerts, K., Herreman, A., Annaert, W., Umans, L., Lübke, T., Lena Illert, A., von Figura, K., and Saftig, P. (2002). The disintegrin/metalloprotease ADAM 10 is essential for Notch signalling but not for α-secretase activity in fibroblasts. Hum. Mol. Genet. *11*, 2615–2624.

Herreman, A., Serneels, L., Annaert, W., Collen, D., Schoonjans, L., and De Strooper, B. (2000). Total inactivation of γ-secretase activity in presenilin-deficient embryonic stem cells. Nat. Cell Biol. *2*, 461–462.

Hoffman, R.C., Jennings, L.L., Tsigelny, I., Comoletti, D., Flynn, R.E., Sudhof, T.C., and Taylor, P. (2004). Structural characterization of recombinant soluble rat neuroligin 1: mapping of secondary structure and glycosylation by mass spectrometry. Biochemistry *43*, 1496–1506.

Horiuchi, K., Miyamoto, T., Takaishi, H., Hakozaki, A., Kosaki, N., Miyauchi, Y., Furukawa, M., Takito, J., Kaneko, H., Matsuzaki, K., et al. (2007). Cell surface colony-stimulating factor 1 can be cleaved by TNF-α converting enzyme or endocytosed in a clathrin-dependent manner. J. Immunol. *179*, 6715–6724.

Huettner, J.E., and Bean, B.P. (1988). Block of N-methyl-D-aspartate-activated current by the anticonvulsant MK-801: selective binding to open channels. Proc. Natl. Acad. Sci. USA *85*, 1307–1311.

Ichtchenko, K., Hata, Y., Nguyen, T., Ullrich, B., Missler, M., Moomaw, C., and Südhof, T.C. (1995). Neuroligin 1: a splice site-specific ligand for β-neurexins. Cell *81*, 435–443.

Inoue, E., Deguchi-Tawarada, M., Togawa, A., Matsui, C., Arita, K., Katahira-Tayama, S., Sato, T., Yamauchi, E., Oda, Y., and Takai, Y. (2009). Synaptic activity prompts γ-secretase-mediated cleavage of EphA4 and dendritic spine formation. J. Cell Biol. *185*, 551–564.

Irie, M., Hata, Y., Takeuchi, M., Ichtchenko, K., Toyoda, A., Hirao, K., Takai, Y., Rosahl, T.W., and Südhof, T.C. (1997). Binding of neuroligins to PSD-95. Science *277*, 1511–1515.

Isokawa, M. (1998). Remodeling dendritic spines in the rat pilocarpine model of temporal lobe epilepsy. Neurosci. Lett. *258*, 73–76.

Janes, P.W., Wimmer-Kleikamp, S.H., Frangakis, A.S., Treble, K., Griesshaber, B., Sabet, O., Grabenbauer, M., Ting, A.Y., Saftig, P., Bastiaens, P.I., and Lackmann, M. (2009). Cytoplasmic relaxation of active Eph controls ephrin shedding by ADAM10. PLoS Biol. *7*, e1000215.

Jorissen, E., Prox, J., Bernreuther, C., Weber, S., Schwanbeck, R., Serneels, L., Snellinx, A., Craessaerts, K., Thathiah, A., Tesseur, I., et al. (2010). The disintegrin/metalloproteinase ADAM10 is essential for the establishment of the brain cortex. J. Neurosci. *30*, 4833–4844.

Kamenetz, F., Tomita, T., Hsieh, H., Seabrook, G., Borchelt, D., Iwatsubo, T., Sisodia, S., and Malinow, R. (2003). APP processing and synaptic function. Neuron *37*, 925–937.

Kawaguchi, N., Horiuchi, K., Becherer, J.D., Toyama, Y., Besmer, P., and Blobel, C.P. (2007). Different ADAMs have distinct influences on Kit ligand processing: phorbol-ester-stimulated ectodomain shedding of Kitl1 by ADAM17 is reduced by ADAM19. J. Cell Sci. *120*, 943–952.

Kenchappa, R.S., Zampieri, N., Chao, M.V., Barker, P.A., Teng, H.K., Hempstead, B.L., and Carter, B.D. (2006). Ligand-dependent cleavage of the P75 neurotrophin receptor is necessary for NRIF nuclear translocation and apoptosis in sympathetic neurons. Neuron *50*, 219–232.

Kim, S.H., Fraser, P.E., Westaway, D., St George-Hyslop, P.H., Ehrlich, M.E., and Gandy, S. (2010). Group II metabotropic glutamate receptor stimulation triggers production and release of Alzheimer's amyloid(β)42 from isolated intact nerve terminals. J. Neurosci. *30*, 3870–3875.

Ko, J., Zhang, C., Arac, D., Boucard, A.A., Brunger, A.T., and Südhof, T.C. (2009). Neuroligin-1 performs neurexin-dependent and neurexin-independent functions in synapse validation. EMBO J. *28*, 3244–3255.

Kochan, L.D., Churn, S.B., Omojokun, O., Rice, A., and DeLorenzo, R.J. (2000). Status epilepticus results in an N-methyl-D-aspartate receptor-dependent inhibition of Ca2+/calmodulin-dependent kinase II activity in the rat. Neuroscience *95*, 735–743.

Kohutek, Z.A., diPierro, C.G., Redpath, G.T., and Hussaini, I.M. (2009). ADAM-10-mediated N-cadherin cleavage is protein kinase C-α dependent and promotes glioblastoma cell migration. J. Neurosci. *29*, 4605–4615.

Koyama, R., Muramatsu, R., Sasaki, T., Kimura, R., Ueyama, C., Tamura, M., Tamura, N., Ichikawa, J., Takahashi, N., Usami, A., et al. (2007). A low-cost method for brain slice cultures. J. Pharmacol. Sci. *104*, 191–194.

Kuhn, P.H., Wang, H., Dislich, B., Colombo, A., Zeitschel, U., Ellwart, J.W., Kremmer, E., Rossner, S., and Lichtenthaler, S.F. (2010). ADAM10 is the physiologically relevant, constitutive α-secretase of the amyloid precursor protein in primary neurons. EMBO J. *29*, 3020–3032.

Kurz, J.E., Moore, B.J., Henderson, S.C., Campbell, J.N., and Churn, S.B. (2008). A cellular mechanism for dendritic spine loss in the pilocarpine model of status epilepticus. Epilepsia *49*, 1696–1710.

Levinson, J.N., and El-Husseini, A. (2007). A crystal-clear interaction: relating neuroligin/neurexin complex structure to function at the synapse. Neuron *56*, 937–939.

Levinson, J.N., Chéry, N., Huang, K., Wong, T.P., Gerrow, K., Kang, R., Prange, O., Wang, Y.T., and El-Husseini, A. (2005). Neuroligins mediate excitatory and inhibitory synapse formation: involvement of PSD-95 and neurexin-1β in neuroligin-induced synaptic specificity. J. Biol. Chem. *280*, 17312–17319.

Marambaud, P., Wen, P.H., Dutt, A., Shioi, J., Takashima, A., Siman, R., and Robakis, N.K. (2003). A CBP binding transcriptional repressor produced by the PS1/ε-cleavage of N-cadherin is inhibited by PS1 FAD mutations. Cell *114*, 635–645.

Marcello, E., Gardoni, F., Mauceri, D., Romorini, S., Jeromin, A., Epis, R., Borroni, B., Cattabeni, F., Sala, C., Padovani, A., and Di Luca, M. (2007). Synapse-associated protein-97 mediates α-secretase ADAM10 trafficking and promotes its activity. J. Neurosci. *27*, 1682–1691.

Mumm, J.S., Schroeter, E.H., Saxena, M.T., Griesemer, A., Tian, X., Pan, D.J., Ray, W.J., and Kopan, R. (2000). A ligand-induced extracellular cleavage regulates γ-secretase-like proteolytic activation of Notch1. Mol. Cell *5*, 197–206.

Nagano, O., Murakami, D., Hartmann, D., De Strooper, B., Saftig, P., Iwatsubo, T., Nakajima, M., Shinohara, M., and Saya, H. (2004). Cell-matrix interaction via CD44 is independently regulated by different metalloproteinases activated in response to extracellular Ca(2+) influx and PKC activation. J. Cell Biol. *165*, 893–902.

Nakahara, S., Tamura, M., Matsuki, N., and Koyama, R. (2009). Neuronal hyperactivity sustains the basal dendrites of immature dentate granule cells: time-lapse confocal analysis using hippocampal slice cultures. Hippocampus *19*, 379–391.

Parent, A.T., Barnes, N.Y., Taniguchi, Y., Thinakaran, G., and Sisodia, S.S. (2005). Presenilin attenuates receptor-mediated signaling and synaptic function. J. Neurosci. *25*, 1540–1549.

Patel, S., Meldrum, B.S., and Fine, A. (1988). Susceptibility to pilocarpine-induced seizures in rats increases with age. Behav. Brain Res. *31*, 165–167.

Prinzen, C., Trümbach, D., Wurst, W., Endres, K., Postina, R., and Fahrenholz, F. (2009). Differential gene expression in ADAM10 and mutant ADAM10 transgenic mice. BMC Genomics *10*, 66.

Reiss, K., Maretzky, T., Ludwig, A., Tousseyn, T., de Strooper, B., Hartmann, D., and Saftig, P. (2005). ADAM10 cleavage of N-cadherin and regulation of cell-cell adhesion and β-catenin nuclear signalling. EMBO J. *24*, 742–752.

Restituito, S., Khatri, L., Ninan, I., Mathews, P.M., Liu, X., Weinberg, R.J., and Ziff, E.B. (2011). Synaptic autoregulation by metalloproteases and γ-secretase. J. Neurosci. *31*, 12083–12093.

Rivera, S., Khrestchatisky, M., Kaczmarek, L., Rosenberg, G.A., and Jaworski, D.M. (2010). Metzincin proteases and their inhibitors: foes or friends in nervous system physiology? J. Neurosci. *30*, 15337–15357.

Saftig, P., and Reiss, K. (2011). The "A Disintegrin And Metalloproteases" ADAM10 and ADAM17: novel drug targets with therapeutic potential? Eur. J. Cell Biol. *90*, 527–535.

Saura, C.A., Servián-Morilla, E., and Scholl, F.G. (2011). Presenilin/γ-secretase regulates neurexin processing at synapses. PLoS ONE *6*, e19430.

Schapitz, I.U., Behrend, B., Pechmann, Y., Lappe-Siefke, C., Kneussel, S.J., Wallace, K.E., Stempel, A.V., Buck, F., Grant, S.G., Schweizer, M., et al. (2010). Neuroligin 1 is dynamically exchanged at postsynaptic sites. J. Neurosci. *30*, 12733–12744.

Scheiffele, P., Fan, J., Choih, J., Fetter, R., and Serafini, T. (2000). Neuroligin expressed in nonneuronal cells triggers presynaptic development in contacting axons. Cell *101*, 657–669.

Shipman, S.L., Schnell, E., Hirai, T., Chen, B.S., Roche, K.W., and Nicoll, R.A. (2011). Functional dependence of neuroligin on a new non-PDZ intracellular domain. Nat. Neurosci. *14*, 718–726.

Siddiqui, T.J., and Craig, A.M. (2011). Synaptic organizing complexes. Curr. Opin. Neurobiol. *21*, 132–143.

Song, J.Y., Ichtchenko, K., Südhof, T.C., and Brose, N. (1999). Neuroligin 1 is a postsynaptic cell-adhesion molecule of excitatory synapses. Proc. Natl. Acad. Sci. USA *96*, 1100–1105.

Südhof, T.C. (2008). Neuroligins and neurexins link synaptic function to cognitive disease. Nature *455*, 903–911.

Sugahara, K.N., Murai, T., Nishinakamura, H., Kawashima, H., Saya, H., and Miyasaka, M. (2003). Hyaluronan oligosaccharides induce CD44 cleavage and promote cell migration in CD44-expressing tumor cells. J. Biol. Chem. *278*, 32259–32265.

Swendeman, S., Mendelson, K., Weskamp, G., Horiuchi, K., Deutsch, U., Scherle, P., Hooper, A., Rafii, S., and Blobel, C.P. (2008). VEGF-A stimulates ADAM17-dependent shedding of VEGFR2 and crosstalk between VEGFR2 and ERK signaling. Circ. Res. *103*, 916–918.

Thyagarajan, A., and Ting, A.Y. (2010). Imaging activity-dependent regulation of neurexin-neuroligin interactions using trans-synaptic enzymatic biotinylation. Cell *143*, 456–469.

Tomita, T., Tokuhiro, S., Hashimoto, T., Aiba, K., Saido, T.C., Maruyama, K., and Iwatsubo, T. (1998). Molecular dissection of domains in mutant presenilin 2 that mediate overproduction of amyloidogenic forms of amyloid β peptides. Inability of truncated forms of PS2 with familial Alzheimer's disease mutation to increase secretion of Aβ42. J. Biol. Chem. *273*, 21153–21160.

Tomita, T., Tanaka, S., Morohashi, Y., and Iwatsubo, T. (2006). Presenilin-dependent intramembrane cleavage of ephrin-B1. Mol. Neurodegener. *1*, 2.

Varoqueaux, F., Jamain, S., and Brose, N. (2004). Neuroligin 2 is exclusively localized to inhibitory synapses. Eur. J. Cell Biol. *83*, 449–456.

Varoqueaux, F., Aramuni, G., Rawson, R.L., Mohrmann, R., Missler, M., Gottmann, K., Zhang, W., Südhof, T.C., and Brose, N. (2006). Neuroligins determine synapse maturation and function. Neuron *51*, 741–754.

Villasana, L.E., Klann, E., and Tejada-Simon, M.V. (2006). Rapid isolation of synaptoneurosomes and postsynaptic densities from adult mouse hippocampus. J. Neurosci. Methods *158*, 30–36.

Weskamp, G., Ford, J.W., Sturgill, J., Martin, S., Docherty, A.J., Swendeman, S., Broadway, N., Hartmann, D., Saftig, P., Umland, S., et al. (2006). ADAM10 is a principal 'sheddase' of the low-affinity immunoglobulin E receptor CD23. Nat. Immunol. *7*, 1293–1298.

Witters, L., Scherle, P., Friedman, S., Fridman, J., Caulder, E., Newton, R., and Lipton, A. (2008). Synergistic inhibition with a dual epidermal growth factor receptor/HER-2/neu tyrosine kinase inhibitor and a disintegrin and metalloprotease inhibitor. Cancer Res. *68*, 7083–7089.

Xu, J., Xiao, N., and Xia, J. (2010). Thrombospondin 1 accelerates synaptogenesis in hippocampal neurons through neuroligin 1. Nat. Neurosci. *13*, 22–24.

Yoda, M., Kimura, T., Tohmonda, T., Uchikawa, S., Koba, T., Takito, J., Morioka, H., Matsumoto, M., Link, D.C., Chiba, K., et al. (2011). Dual functions of cell-autonomous and non-cell-autonomous ADAM10 activity in granulopoiesis. Blood *118*, 6939–6942.

Zhang, C., Milunsky, J.M., Newton, S., Ko, J., Zhao, G., Maher, T.A., Tager-Flusberg, H., Bolliger, M.F., Carter, A.S., Boucard, A.A., et al. (2009). A neuroligin-4 missense mutation associated with autism impairs neuroligin-4 folding and endoplasmic reticulum export. J. Neurosci. *29*, 10843–10854.

Zhou, H.M., Weskamp, G., Chesneau, V., Sahin, U., Vortkamp, A., Horiuchi, K., Chiusaroli, R., Hahn, R., Wilkes, D., Fisher, P., et al. (2004). Essential role for ADAM19 in cardiovascular morphogenesis. Mol. Cell. Biol. *24*, 96–104.

Zhou, B.B., Peyton, M., He, B., Liu, C., Girard, L., Caudler, E., Lo, Y., Baribaud, F., Mikami, I., Reguart, N., et al. (2006). Targeting ADAM-mediated ligand cleavage to inhibit HER3 and EGFR pathways in non-small cell lung cancer. Cancer Cell *10*, 39–50.